Carbohydrate Detection

DOI: 10.1002/anie.201001220

# Assessment of Tumor Metastasis by the Direct Determination of Cell-Membrane Sialic Acid Expression**

*Akira Matsumoto, Horacio Cabral, Naoko Sato, Kazunori Kataoka, and Yuji Miyahara**

Sialic acid (SA) is an anionic monosaccharide that frequently occurs at the termini of glycan chains and provides many opportunities for the assessment of both normal and pathological cell processes. It is generally present in tumor-associated carbohydrate antigens, including those clinically approved as tumor markers. Accordingly, the overexpression of SA on cell membranes has been implicated in the malignant and metastatic phenotypes of various types of cancer.[1] Therefore, SA is an important molecular target for diagnostic and therapeutic approaches. The installation of SA-specific ligands enables reagents to target highly sialylated or tumor cells.[2] Alternatively, monitoring of the cell-surface expression of SA should provide rational indexes of dynamic changes in pathological conditions and other SA-associated biological events. We previously developed a method for the potentiometric detection of SA by exploiting the reversible and specific nature of the binding between phenylboronic acid (PBA) and SA. A gold electrode modified with PBA and with a carefully optimized dissociation constant (or $pK_a$ value) was able to quantify SA present in the free state as well as cell-surface SA under physiological aqueous conditions.[3] The observed ability of the electrode to differentiate altered levels of SA expression on the surface of rabbit erythrocytes is relevant to the diagnosis of insulin-dependent diabetes mellitus (IDDM). The approach provided a new rationale for the label-free, noninvasive (enzyme-free and operative on living cells), and real-time determination of SA. Herein we show that the technique can also be applied to the analysis of tumor malignancy and the degree of metastasis.

PBA derivatives are able to form reversible cyclic boronates with 1,2-diols, 1,3-diols, and polyols: hallmark structures of the majority of glycans.[4] Because of this property, PBA has quite a history as a synthetic ligand for these molecules.[5] It is usually observed that these complexes have a stabilizing effect only if PBA is disassociated (at pH values above the $pK_a$ value),[6] whereas those formed between nondissociated PBA and sugars are unstable with high susceptibility to hydrolysis.[4d] However, as an exception, a complex formed between nondissociated PBA and SA is remarkably stable owing to its special binding modalities, some aspects of which have been clarified previously.[7] As a result, a PBA with an appropriate $pK_a$ value can provide a molecular basis for selective recognition of SA among other saccharides under physiological conditions (see the Supporting Information).

A procedure for the surface modification of a gold electrode with PBA was described previously.[3] Briefly, a self-assembled monolayer (SAM) of 10-carboxy-1-decanethiol was first formed on a gold electrode. Next, a reaction between the terminal carboxyl groups and 3-aminophenylboronic acid resulted in the introduction of *meta*-amide-substituted PBA on the SAM surface. Both quartz crystal microbalance (QCM) and ellipsometric measurements confirmed stoichiometric monolayer formation at each step of the reaction (see the Supporting Information). The surface PBA moiety had an apparent $pK_a$ value of about 9.5, as judged from pH-dependent changes in its threshold voltage ($V_T$; see the Supporting Information). We could therefore safely conclude that it was not dissociated at the physiological pH value (7.4) and would be SA-specific under such conditions.

The electrode was then linked to a field-effect-transistor (FET) gate for the real-time monitoring of charge-density changes on the electrode. In this configuration, a carboxyl anion of SA can be detected as a positive-direction shift of the $V_T$ value of the FET. Owing to the nature of the field effect, FET-based charge detection is possible only within a distance corresponding to the electrical double layer or the Debye length, which is no greater than a few nanometers even under conditions of minimized ionic strength.[8] This requirement should be compatible with the purpose of detecting cell-surface SA moieties, which generally dominate the termini of the glycan chains, as described earlier. Besides, the tumor- or metastasis-associated overexpression of SA is usually found in the form of polysialylation. Such a sequential arrangement of target SA units (as an SA homopolymer) on the glycan-chain termini may help to enable the precise reflection of altered levels of SA expression. Moreover, the fact that the technique is limited to short detection distances could beneficially restrict charge detection to molecules that are truly (covalently) bound to the electrode surface within the vicinity of the Debye length (i.e., PBA-bound SA) and exclude other charges bound through nonspecific or non-covalent interactions.

To demonstrate the ability of the electrode to assess malignancy or metastasis of a tissue specimen, metastatic murine melanoma cells expressing luciferase (B16-F10-Luc-

[*] Dr. A. Matsumoto, Dr. H. Cabral, N. Sato, Dr. K. Kataoka, Dr. Y. Miyahara
Centre for NanoBio Integration, The University of Tokyo
Hongo 7-3-1, Bunkyo-ku, Tokyo (Japan)
Fax: (+81) 29-860-4506
E-mail: miyahara.yuji@nims.go.jp
Dr. Y. Miyahara
Biomaterials Center and International Center for Materials Nanoarchitectonics, National Institute for Materials Science
Namiki 1-1, Tsukuba, Ibaraki 305-0044 (Japan)

[**] This research was supported in part by the JST, CREST.

Supporting information for this article is available on the WWW under http://dx.doi.org/10.1002/anie.201001220.

G5) were utilized for their ability to almost specifically metastasize to healthy lungs of mice after intravenous injection.[9] This system enabled the facile preparation of tumoral lung specimens with various degrees of metastasis simply through control of the incubation time after each injection. Herein, the degree of metastasis denotes a number fraction relating B16-F10-Luc-G5 to a total cell population (B16-F10-Luc-G5+healthy pneumocyte), which could be determined on the basis of bioluminescence for a given cell suspension. Incubation for 10 and 17 days after the injection provided tumoral lung specimens with 15 and 30% metastasis, respectively (Figure 1a,b). These samples were subjected to SA-expression analysis with the electrode. Healthy pneumocytes (as a model for 0% metastasis) and cultured (pure) B16-F10-Luc-G5 (as a model for 100% metastasis) were also analyzed for comparison. An independent enzymatic analysis (with a commercial kit: SIALICQ, Sigma) had indicated that the amount of SA present on B16-F10-Luc-G5 was about four times as high as the amount of pneumocytes: $1120 \pm 30$ and $270 \pm 18$ pmol/$10^6$ cells, respectively ($n = 3$). Figure 1c shows microscopic images of a slice of the 30% metastasized lung. In the dark regions corresponding to the melanoma cells in the transmittance image (top), stronger staining of SA with FITC-labeled wheat-germ agglutinin was observed (middle and bottom) than in the case of healthy pneumocytes (brighter regions in Figure 1c, top and bottom, or dark regions in Figure 1c, middle), in accordance with the above-mentioned difference in the surface SA densities of these cell types.

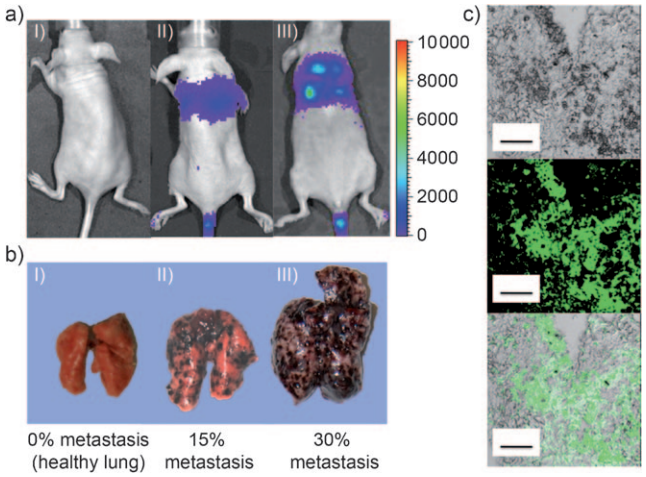


***Figure 1.*** a) Bioluminescent images of Balb/c nu/nu mice with graded degrees of lung metastasis following intravenous injection (into the tail vein) of B16-F10-Luc-G5: I) 0 (healthy lung), II) 15 (at day 10), and III) 30% metastasis (at day 17). b) Macroscopic images of the lungs of each specimen showing B16-F10-Luc-G5 metastasized tumors. c) Microscopic images of a slice of the 30% metastasized lung specimen. Top: transmittance image, middle: fluorescence image taken following the staining of SA with FITC–WGA, bottom: superposition of the top and middle images. Scale bars: 100 μm. FITC = fluorescein isothiocyanate, WGA = wheat-germ agglutinin.

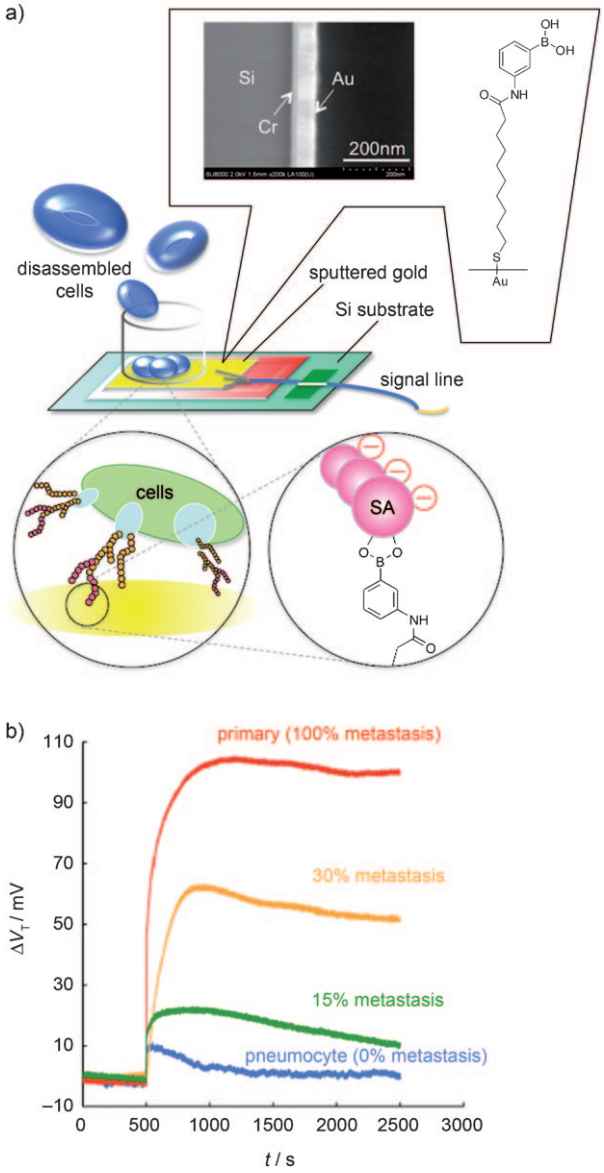


***Figure 2.*** a) Schematic representation of potentiometric SA detection with a PBA-modified gold electrode. An SEM image of a cross-section of the electrode is shown at the top next to the chemical structure of the PBA-modified self-assembled monolayer introduced onto the electrode surface. b) Change in the threshold voltage ($V_T$) of the PBA-modified FET as a function of time upon the addition of cell suspensions ($10^6$ cells $mL^{-1}$) with various degrees of metastasis.

Figure 2a summarizes the principle behind the detection of cell-surface glycan-chain SA with the PBA-modified gold electrode. Figure 2b shows representative profiles of the $V_T$ response of the electrode with respect to time upon the addition of cell suspensions with various degrees of metastasis. In all cases, the $V_T$ value increased promptly upon the addition of the cells, presumably as a result of the detection of negatively charged SA moieties. The effect of other intrinsic disparities between healthy pneumocytes and the melanoma, such as size, mechanical properties of the membrane, and clustering (although the cells were disassembled with a cell strainer: see the Experimental Section), cannot be completely excluded from potential factors contributing to alteration of the signal, but these factors are likely to be small considering

  

the previously demonstrated remarkable SA-specificity of the PBA-modified electrode.[3] This prompt increase in the $V_T$ response was followed by a trend toward recovery, the rate of which was lower as the degree of metastasis and the cell concentration increased, a feature probably related to the site-density-dependent stability of PBA–SA binding. In each case, a data point at 0.5 h (1800 s) after the addition of the cells was defined as the equilibrium $V_T$ shift.

Figure 3a summarizes the equilibrium $V_T$ shift as a function of the degree of metastasis for various cell concentrations (along with data sets for cultured melanoma and healthy pneumocytes); Figure 3b shows a control series for which an electrode without PBA modification was used. Figure 3c indicates enzymatically determined amounts of SA that should be present in the system, also as a function of the degree of metastasis. Together, the profiles in Figure 3a demonstrate that an advancement of metastasis in living tissue can be assessed with the PBA-modified electrode. Importantly, for this assessment, the known-count living-cell suspensions were simply placed on the electrode without any enzymatic, labeling, or lethal procedures, which are unavoidable in any other existing determination methods.

In summary, a PBA-modified electrode with a properly controlled pKa value can differentiate the degree of tumor metastasis through the detection of cell-membrane SA. The technique can be readily extended to other primary/tissue systems if their cell-number–$V_T$ relationships are predetermined. Such an approach may serve as a remarkably straightforward and quantitative adjunct to the histological evaluation of tumor malignancy and metastatic potential during intra- or postoperative diagnosis.

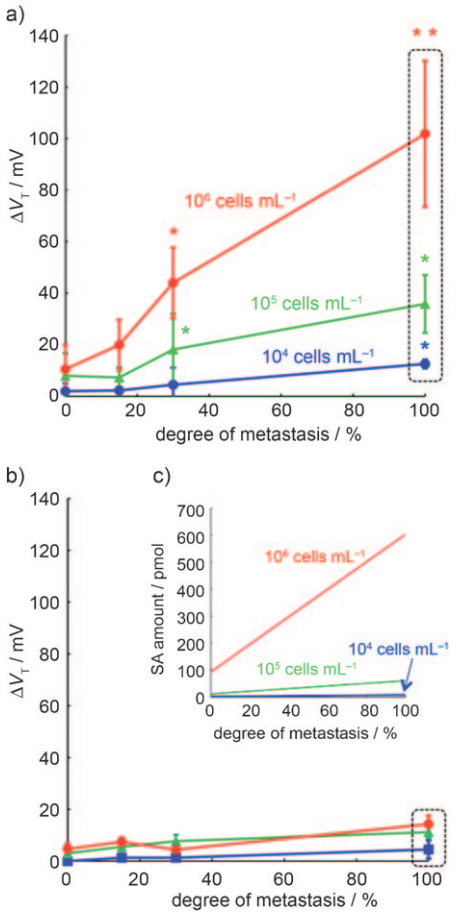


***Figure 3.*** Equilibrium $V_T$ shifts (at 1800 s after each addition) found by adding cell suspensions to: a) PBA-modified and b) non-PBA-modified gold electrodes as a function of the degree of metastasis for various cell concentrations. Data sets for the 100% tumoral fraction (dashed boxes) were obtained from cultured B16-F10-Luc-G5 (no pneumocytes), whereas those for 0% were from healthy pneumocytes. Data are expressed as averages ± standard deviation ($n = 6$, * and ** indicate $p < 0.05$ and $p < 0.01$, respectively, versus 0% metastasis for the same cell concentrations). c) Amount of SA present per electrode well under equivalent conditions to those investigated in (a) and (b), as determined by an enzymatic method with a commercial kit (SIALICQ, Sigma).

## *Experimental Section*

A gold electrode (4 × 4 mm$^2$) was fabricated by the sputter deposition of an adhesion layer of chromium (10 nm) and then a gold layer (90 nm, 99.99% purity) on a silicon substrate. The surface was subjected to plasma cleaning in an oxygen plasma reactor (Yamato) for 90 s with a power of 300 W and an oxygen pressure of 200 Pa, immersed immediately thereafter in a 10 mM solution of 10-carboxy-1-decanethiol in ethanol, and incubated for 24 h at room temperature. After repeated rinses and sonication in pure ethanol for 5 min, the electrode was immersed in a 100 mM solution of 1-ethyl-3-(3-dimethylaminopropyl)carbodiimide hydrochloride in *N*,*N*-dimethylformamide (DMF) for 1 h to activate the SAM terminal carboxyl groups. After removal of the solution, the electrode was transferred to a 1:1 (v/v) mixture of DMF and 1M aqueous NaOH containing a 3-aminophenylboronic acid (20 mM). The condensation reaction was continued for 24 h at room temperature.

Balb/c nu/nu mice (female) were inoculated intravenously through the tail vein with metastatic murine melanoma cells expressing luciferase (B16-F10-Luc-G5, Xenogen; $10^6$ cells mL$^{-1}$). In vivo bioluminescent imaging was performed with an IVIS imaging system (Xenogen). Mice were sacrificed 10 and 17 days postinjection, and their lungs were collected. For the determination of tumoral fractions in each tissue specimen, tissues were disassembled into single cells with a cell strainer (BD Falcon). To minimize damage to cell-surface carbohydrates, no enzymatic treatment was conducted. Subsequently, the total cell numbers were determined by using a NucleoCounter (ChemoMetec A/S), and the fractions of B16-F10-Luc-G5 were quantified bioluminescently in photons per second by using the Living Image software. All animal experiments had been approved by the ethics committee of The University of Tokyo.

Surface characterization of the PBA-modified gold electrode is provided in the Supporting Information along with detailed procedures for the use of the electrode as an extended gate for FET, potentiometric measurements, the colorimetric determination of SA (with a commercial kit), and a histological assay of a lung specimen.

Received: March 1, 2010
Published online: June 23, 2010

**Keywords:** cancer · carbohydrates · field-effect transistors · self-assembled monolayers · potentiometric detection

[1] a) M. Fukuda, *Cancer Res.* **1996**, *56*, 2237–2244; b) C. R. Bertozzi, L. L. Kiessling, *Science* **2001**, *291*, 2357–2364; c) S. Hakomori, *Cancer Res.* **1985**, *45*, 2405–2414; d) M. Mammen, S. K. Choi, G. M. Whitesides, *Angew. Chem.* **1998**, *110*, 2908–

  

2953; *Angew. Chem. Int. Ed.* **1998**, *37*, 2754 – 2794; e) A. Raz, W. L. McLellan, I. R. Hart, C. D. Bucana, L. C. Hoyer, B. A. Sela, P. Dragsten, I. J. Fidler, *Cancer Res.* **1980**, *40*, 1645 – 1651; f) L. Dobrossy, Z. P. Pavelic, R. J. A. Bernacki, *Cancer Res.* **1981**, *41*, 2262 – 2266; g) A. Passaniti, G. W. Hart, *J. Biol. Chem.* **1988**, *263*, 7591 – 7603.

[2] a) G. Lemieux, K. J. Yarema, C. L. Jacobs, C. R. Bertozzi, *J. Am. Chem. Soc.* **1999**, *121*, 4278 – 4279; b) L. Frullano, J. Rohovec, S. Aime, T. Maschmeyer, M. I. Prata, J. J. P. de Lima, C. F. G. C. Geraldes, J. A. Peters, *Chem. Eur. J.* **2004**, *10*, 5205 – 5217; c) K. Djanashvili, G. A. Koning, A. J. G. M. van der Meer, H. T. Wolterbeek, J. A. Peters, *Contrast Media Mol. Imaging* **2007**, *2*, 35 – 41; d) E. Uchimura, Y. Miyazaki, H. Otsuka, T. Okano, Y. Sakurai, K. Kataoka, *Biotechnol. Bioeng.* **2001**, *72*, 307 – 314; e) L. K. Mahal, N. W. Charter, K. Angata, M. Fukuda, D. E. Koshland, Jr., C. R. A. Bertozzi, *Science* **2001**, *294*, 380 – 382; f) I. Kijima-Suda, Y. Miyamoto, S. Toyoshima, M. Itoh, T. Osawa, *Cancer Res.* **1986**, *46*, 858 – 862.

[3] A. Matsumoto, N. Sato, K. Kataoka, Y. Miyahara, *J. Am. Chem. Soc.* **2009**, *131*, 12022 – 12023.

[4] a) J. Boeseken, *Adv. Carbohyd. Chem.* **1949**, *4*, 189 – 210; b) A. B. Foster, *Adv. Carbohyd. Chem.* **1957**, *12*, 81 – 115; c) S. Aronoff, T. Chen, M. Cheveldayoff, *Carbohydr. Res.* **1975**, *40*, 299 – 309; d) J. P. Lorand, J. O. Edwards, *J. Org. Chem.* **1959**, *24*, 769 – 774.

[5] a) T. D. James, K. R. A. S. Sandanayake, S. Shinkai, *Angew. Chem.* **1996**, *108*, 2038 – 2050; *Angew. Chem. Int. Ed. Engl.* **1996**, *35*, 1910 – 1922; T. D. James, K. R. A. S. Sandanayake, S. Shinkai, *Nature* **1995**, *374*, 345 – 347; T. D. James, K. R. A. S. Sandanayake, R. Iguchi, S. Shinkai, *J. Am. Chem. Soc.* **1995**, *117*, 8982 – 8987; b) K. Kataoka, H. Miyazaki, M. Bunya, T. Okano, Y. Sakurai, *J. Am. Chem. Soc.* **1998**, *120*, 12694 – 12695; c) A. Matsumoto, K. Yamamoto, R. Yoshida, K. Kataoka, Y. Miyahara, *Chem. Commun.* **2010**, *46*, 2203 – 2205.

[6] a) A. Matsumoto, S. Ikeda, A. Harada, K. Kataoka, *Biomacromolecules* **2003**, *4*, 1410 – 1416; b) M. Dowlut, D. G. Hall, *J. Am. Chem. Soc.* **2006**, *128*, 4226 – 4227.

[7] a) H. Otsuka, E. Uchimura, H. Koshina, T. Okano, K. Kataoka, *J. Am. Chem. Soc.* **2003**, *125*, 3493 – 3502; b) K. Djanashvili, L. Frullano, J. A. Peters, *Chem. Eur. J.* **2005**, *11*, 4010 – 4018.

[8] a) P. Bergveld, *Sens. Actuators A* **1996**, *56*, 65 – 73; P. Bergveld, *Biosens. Bioelectron.* **1991**, *6*, 55 – 72; b) M. J. Schöning, A. Poghossian, *Analyst* **2002**, *127*, 1137 – 1151, and references therein; c) E. Stern, R. Wagner, F. J. Sigworth, R. Breaker, T. M. Fahmy, M. A. Reed, *Nano Lett.* **2007**, *7*, 3405 – 3409.

[9] a) I. J. Fidler, *Nature New Biol.* **1973**, *242*, 148 – 149; b) R. S. Parhar, P. K. Lala, *J. Exp. Med.* **1987**, *165*, 14 – 28; c) M. Edinger, Y. A. Cao, Y. S. Hornig, D. E. Jenkins, M. R. Verneris, M. H. Bachmann, R. S. Negrin, C. H. Contag, *Eur. J. Cancer* **2002**, *38*, 2128 – 2136.

  